A Photoelectric Technique for Measuring Lightning-Channel Propagation Velocities from a Mobile Laboratory

DOUGLAS M. MACH* AND W. DAVID RUST

NOAA/National Severe Storms Laboratory, Norman, Oklahoma

(Manuscript received 28 March 1988, in final form 16 October 1988)

ABSTRACT

We have developed a device to measure lightning-channel propagation velocities. It consists of eight solid state silicon photodetectors mounted behind precision horizontal slits in the focal plane of a 50-mm lens on a 35-mm camera body. Each detector has a 0.1° vertical field of view that is separated from adjacent detector slits by 2.8°. The horizontal field-of-view for each detector is 41° and the total vertical field of view for the device is 21°. The signal from each detector is amplified by a circuit with a 10%–90% rise time of 0.6 μs and an equivalent decay time of 400 μs. The eight photodetector pulses, IRIG-B time, and slow and fast electric field change waveforms are recorded on a 14-track analog tape recorder with an upper frequency response of 1.0 MHz and a maximum dynamic interchannel timing error of 0.6 μs. To provide images of lightning geometry and permit time-to-thunder measurements, color video and sound are recorded with a standard VHS video cassette recorder. The return stroke velocity (RSV) device, video camera, and microphone are installed and coaxially aimed in an environmental enclosure on a remotely controlled pan-tilt unit atop our mobile laboratory, permitting the recording of lightning signals at remote sites and while mobile. To evaluate the performance of the RSV device, we have analyzed 12 natural return strokes from Alabama, Florida, and Oklahoma and 4 return strokes triggered at the Kennedy Space Center, Florida. The velocities we determined vary from 1.2 to 2.5×10^8 m s^{-1}, with an average of 1.7×10^8 m s^{-1} $\pm$ 0.8×10^8 m s^{-1}. From comparisons of our results to those of a streaking camera, we find no significant differences between the velocities obtained from the same strokes with the two systems. We also find no differences between the characteristics of the pulses or the velocities calculated from them while the RSV device is moving or stationary.

1. Introduction

The return stroke velocity is a fundamental parameter of cloud-to-ground lightning. This is true with respect to the various return stroke models because the stroke velocity, especially over roughly the first 100 m of the lightning-channel, is necessary for estimating currents (Uman and McLain 1969: Uman et al. 1973, 1975; Leise and Taylor 1977; Lin et al. 1980; Master et al. 1981). Return stroke velocities, however, are difficult to measure owing to their very high values (Idone and Orville 1982). Most previous measurements have been based on data from some form of streaking camera (Schonland and Collens 1934; Schonland et al. 1935; McEachron 1939; Boyle and Orville 1976; Orville et al. 1978). The streaking camera technique has several problems associated with it. The film is mounted on a drum that is rotated at a very high rate; the result is that the spinning drum is hazardous to nearby personnel and requires that the camera and platform be very stable. This eliminates the possibility of operating the camera while mobile. Because the streaking camera uses photographic film, it can only be exposed for a few seconds in daylight before the film is fogged. Filters can be used to lessen this problem, but may bias the velocities to lower values (Idone and Orville 1982). Each film load can record only a few return strokes before it must be replaced. The time spent reloading the camera can result in loss of data. The technique is also limited in a practical way by the high cost of the camera and complicated analysis needed to obtain velocities. Although researchers have been measuring the return stroke velocity for over 50 years with streaking cameras, there have been only about 200 measurements of return stroke velocities published. Also, the reported values vary over an order of magnitude (Boyle and Orville 1976), and many of these measurements were obtained from triggered lightning that may not have the same characteristics as natural lightning.

A more recent technique utilizes time of arrival differences at photodetectors (Radda and Krider 1974; Hubert and Mouget 1981; Kawasaki et al. 1985). Although this technique solves several of the problems

* Present affiliation: Johnson Research Center, The University of Alabama in Huntsville, Huntsville, Alabama.

Corresponding author address: Dr. Douglas M. Mach, Kenneth E. Johnson Research Center, Atmospheric Science and Remote Sensing Laboratory, R.I. Box 212, The University of Alabama in Huntsville, Huntsville, AL 35899.

© 1989 American Meteorological Society

Unauthenticated | Downloaded 05/07/21 08:15 PM UTC

associated with the streaking camera, each instrument using this technique could only determine a single velocity and very little data have been published from the use of these instruments. In addition, these instruments have not utilized the full potential of the method. Because of the small size, ease of operation, and durability of the components, this technique is ideal for mobile use to increase the measurement opportunities greatly. Therefore, we decided to develop a new instrument to address the unresolved issues related to return stroke velocity characteristics. These include 1) possible geographical differences in return stroke velocities that seem to be indicated in magnetic and electric field measurements of lightning (MacGorman et al. 1984), 2) the unknown velocity of naturally occurring 'positive' return strokes, i.e., those that effectively lower positive charge to earth, and 3) the variation of the return stroke velocity along the lightning channel.

In addition, we will be able to use the photoelectric and electric field data to measure the variation of the light intensity along the lightning channel (Jordan and Uman 1983), measure the velocity of various features on the return stroke optical signal, and explore any relations between the return stroke velocity and peak current (Lundholm 1957). Preliminary results indicate that our RSV device also detects dart leaders (Fig. 1), which will allow us to examine dart leader characteristics and their relationship to the overall cloud-to-ground flash.

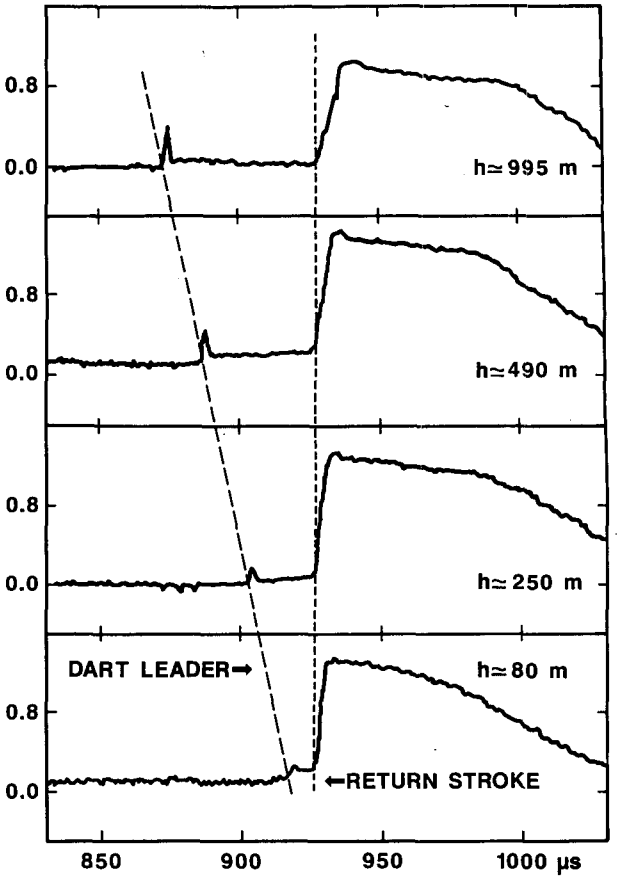

FIG. 1. RSV device voltage out versus time from 4 m channel segments of a natural subsequent return stroke. The detectors are at heights of 80, 250, 490, and 995 m above the ground. The flash occurred on julian date 86 194 at the time 2038:18.868 CST. Note that both dart-leader and return-stroke optical pulses are present.

2. Description of return stroke velocity measuring device

a. Mechanical and optical components

The return stroke velocity (RSV) measuring device consists of electronics connected to an array of solid state silicon photodetectors that are mounted behind a precision horizontal slit assembly in the focal plane of a lens. The precision slits are formed by a three-step process. First, a line drawing is produced that consists of eight horizontal, parallel lines. Details are shown in Fig. 2. The drawing is photographed with a high-contrast, black-and-white film (Kodak Kodalith Ortho Film, Type 3) such that the drawing area completely fills the camera image field with the lines parallel to the top and bottom edges of the film. When developed, the film produces a strip with eight clear and precise 0.1-mm by 36-mm slits, vertically separated by 2.45-mm opaque sections as shown in negative in Fig. 2. This method allows the inexpensive production of precision slits. The one disadvantage of this method is that if the RSV device is aimed at the sun, the film can be pitted by burns. Our experience is that this is not a major disadvantage if the film is checked before each mobile deployment.

The solid state silicon photodetectors are behind the slits. Each detector level consists of two high-speed, blue-enhanced, planar detectors (PBHL-52, manufactured by Advanced Detector Technology), which have the approximate spectral response shown in Fig. 3. The 20-mm by 5-mm detectors are butted together to form a 40-mm by 5-mm detector that completely covers the horizontal dimension of one slit film. Eight of these detectors are produced, one for each slit in the film.

The detectors are mounted to, but electrically isolated from, a grounded aluminum backing plate (Fig. 4), so that each detector is exposed to only one slit. The slit film is mounted to a raised section of the backing plate so that the film just touches the edge of the detectors. This forms a light shield so that signals intended for one detector do not reach adjacent ones. The plate fits securely in the camera body so that the slits are in the image plane of the camera lens. A pin in the back of the camera body fits into a hole in the backing plate so that the slits can be aligned precisely relative to the film guide in the camera body. We use a 50-mm lens on the camera body, which results in each detector having a vertical field of view of 0.1° and a horizontal field of view of 41°. Adjacent detectors are separated vertically by 2.8° so that the total vertical

Unauthenticated | Downloaded 05/07/21 08:15 PM UTC

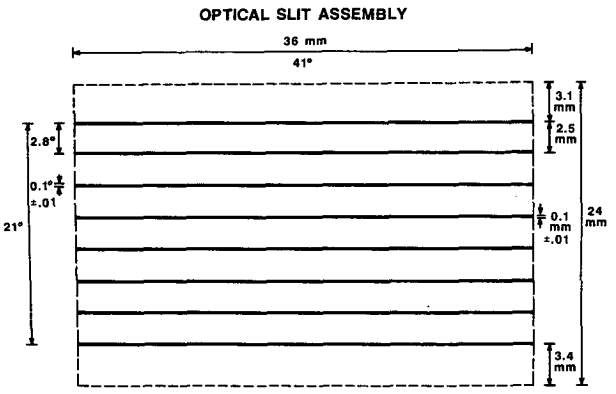

FIG. 2. Diagram of optical slit film used in focal plane of lens on a 35-mm camera body. Tolerances of dimensions are ±0.01 mm, with resulting accuracies in degrees of ±0.01°. The dimensions in degrees are for a 50-mm lens. The optical slit film is from the 10× reduction of an original drawing that consists of horizontal lines centered within a 360-mm by 240-mm drawing area, 1.0 mm wide by 360 mm long and separated (center to center) by 24.5 mm.

field of view of the device is 21°, as depicted in Fig. 5. The angular values can be varied by using lenses with different focal lengths.

b. Electronic components

The detectors are back-biased for faster photoconductive operation, which results in a 10%–90% rise time of <0.1 μs for the current output from the detectors. The current output of each detector is converted to a voltage and amplified by a circuit (Fig. 6) with an overall frequency response of 300 Hz to about 800 kHz (Fig. 7). The frequency response is determined by modulating the optical output of a light-emitting diode with a sinusoidal signal and measuring the relative response of each detector and amplifier circuit. The 10%–90% rise time of the detector plus the amplifier circuit

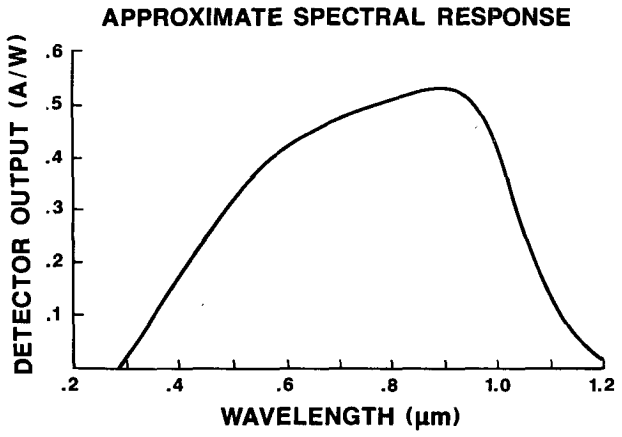

FIG. 3. Spectral response (from manufacturer's specifications) of the optical detectors used in RSV device.

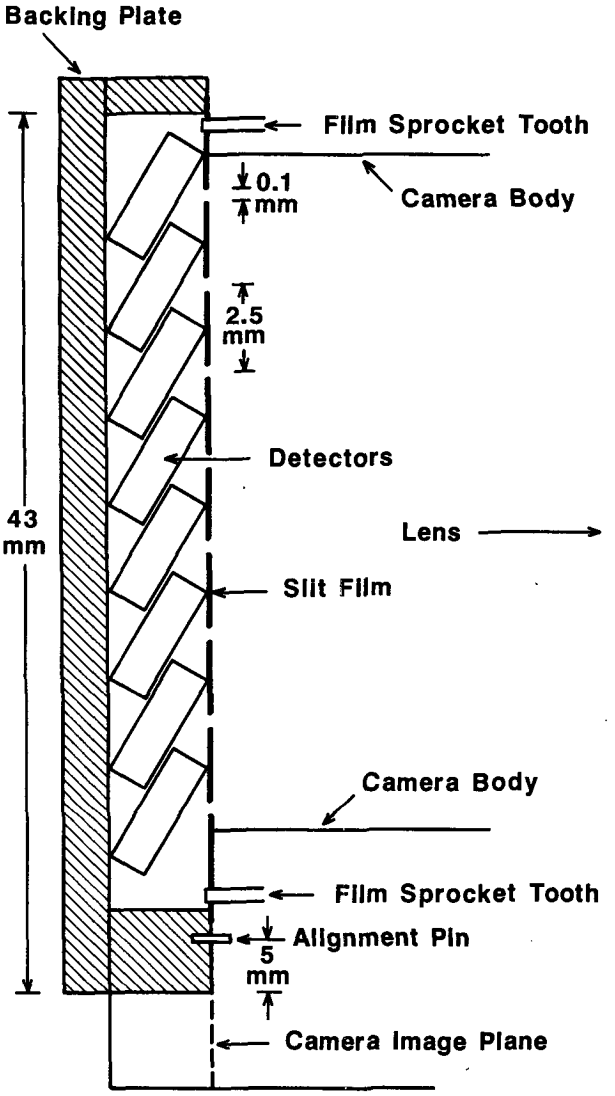

FIG. 4. Mounting of slit film, detectors, and backing plate in RSV device. For precise positioning, the film is aligned with the film guide teeth and the plate with an alignment pin extending from the back of the camera body. The back cover of the camera is permanently removed. The lens is out of view to the right of the drawing.

is 0.6 μs and is determined by using a pulsed signal from a light-emitting diode with a risetime of less than 80 ns. We set the 90%–10% decay time of the circuit to 400 μs so that constant and slowly varying light levels do not saturate the electronics. This allows for the collection of velocity data during daylight and also in the presence of most artificial light sources.

The pulses from the RSV optical detectors, slow and fast electric field change signals, and IRIG-B time code are recorded on a 14-track, wideband II (Fairchild Weston, Model 80) analog tape recorder. The tape recorder is operated at 23.6 cm s^{-1} (60 ips) and loaded with 2800 m (9200 ft) of tape for continuous data collection times of 30 min interspersed with tape-changing

Unauthenticated | Downloaded 05/07/21 08:15 PM UTC

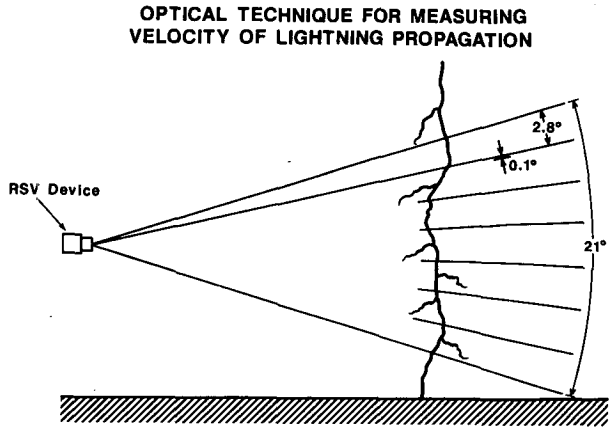

FIG. 5. Representation of a cloud-to-ground stroke in the vertical field of view of RSV device. The angular dimensions are for a 50-mm lens.

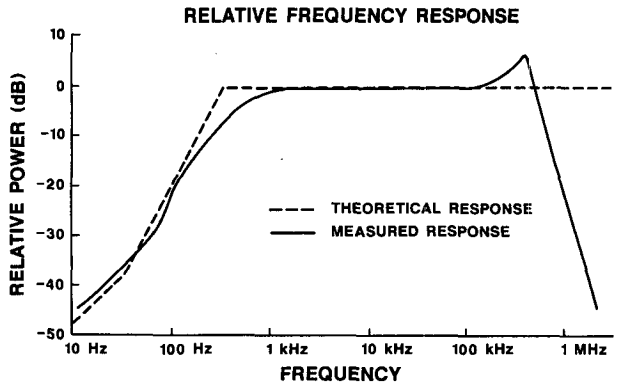

FIG. 7. Frequency response of RSV device. The dashed line is the theoretical response obtained from circuit analysis and the solid line is the measured response obtained by pulsing a light-emitting diode in front of one slit (see text for details.)

times of 1–2 min. At this tape speed, the recorder has a frequency response of 250 Hz to 1 MHz for direct record (DR) channels and 0 Hz to 250 kHz for frequency-modulated (FM) channels. The RSV optical and the fast electric field change signals are recorded on DR channels, and the other instruments are recorded on FM channels. To maximize RSV device interchannel timing accuracy, we record all but one of the optical detector channels on a single headstack. In this configuration, the random interchannel timing error (also called jitter) between the center track and the one outside track is 0.6 μs, but between adjacent tracks is only 0.2 μs (Table 1).

Timing accuracies are determined by recording simultaneous pulses on all recorder channels used for the RSV device, digitizing the pulses at least twenty times, and calculating the average time slip between tracks, i.e., the systematic timing errors. The standard deviations of the time slip are then used to calculate the average 2σ errors (or jitter) between the tracks (Table 1). We measure the average and random errors between all the tracks that we use in our analysis. Only a representative set of 6 of the possible 21 errors are presented in Table 1. In all cases the errors we measured are less than the maximum listed in the recorder specifications (Table 1). The average time slips are used to correct the time difference between the arrival times of the optical signals at each slit in the velocity determinations. Although the systematic errors are larger than the random-jitter errors, the systematic errors can be corrected. The random-jitter errors are the major limiting factor on the time interval we can measure accurately.

c. *Monitoring and aiming components*

To provide images of the lightning geometry and time-to-thunder measurements, picture and sound

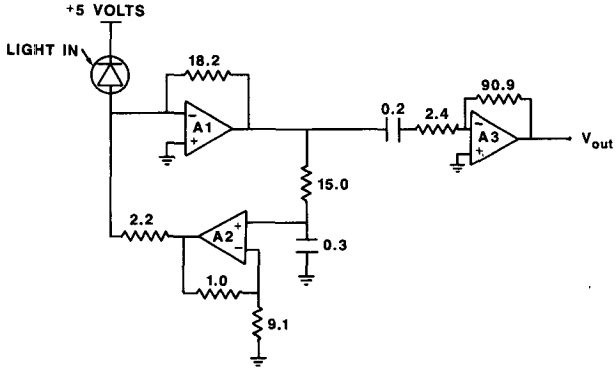

FIG. 6. Optical circuit for RSV device. All resistors shown are in kilohms (kΩ) and all capacitors shown are in microfarads (μF). Amplifiers A1 and A2 are high bandwidth, TP-1322 operational amplifiers manufactured by Teledyne–Philbrick. The amplifier A2 is a low noise OPA-2111 operational amplifier manufactured by Burr–Brown. Not shown are a 680 Ω resistor and a 470 pF capacitor connected in series and placed across the inputs of A1 for amplifier stability.

TABLE 1. Random and systematic errors between one outside (#1) and other tracks of the tape recorder. The center track is #7. The first column is the channel pair that we used to determine the random error. The next two columns are the random errors (2σ of jitter) between each pair. The second column is our calculated value, and the third is the manufacturer's specification. The last column is the average measured systematic time difference between channel pairs. Only a representative set of the 21 possible error combinations are tabulated here (all were calculated). The values shown are typical and are the ones we use in our analysis.

Channel Pair	2σ Timing Errors (μs)		Time Slip (μs)
	Measured	Specified	
1–3	0.2	0.3	0.2
1–5	0.4	0.7	0.5
1–7	0.6	1.0	0.7
1–9	0.8	1.3	1.0
1–11	1.1	1.7	1.3
1–13	1.3	2.0	1.7

Unauthenticated | Downloaded 05/07/21 08:15 PM UTC

from a Panasonic WV-3150 color video camera with a Newvicon S-4131 tube and the standard attached microphone are recorded on a VHS video cassette recorder. The RSV device and video camera are installed and coaxially aimed in an environmental enclosure on a remotely controlled pan-tilt unit mounted atop our mobile laboratory. This allows the RSV device to be pointed to any azimuth at elevation angles of +40° to −20° from the horizon. The enclosure has a windshield wiper, which we found necessary for high-quality video images during rain. For exact determination of the relative slit positions on the video image, we record the locations of the right and left edges of the detector slits on the video image field. We determine the edges by displaying each optical channel output on an oscilloscope and noting on the audio track the locations where the light from a distant strobe is just detected by each channel. The video camera, RSV device, and associated instrumentation are secured and configured to acquire data while moving.

3. RSV device operation and data analysis

As we approach a storm, we activate the mobile laboratory instrumentation to monitor lightning activity. From lightning observations reported by crew members, the RSV device and color video camera are aimed at the area of frequent tall lightning, with the RSV positioned so that the lowest detector slit is below the horizon. We use this positioning of the RSV device to ensure that the lowest section of close lightning is observed. The video camera and RSV device are reaimed continually to keep them pointed towards the maximum ground flash activity as the storm develops and the heading of the mobile lab changes.

The general procedure for flash analysis is straightforward and can be used for leader as well as return-stroke velocities. The video data are examined to find the time of unobstructed cloud-to-ground flashes. We then digitize the optical pulses from the resultant strokes in pairs at a sampling rate of 2.5 MHz. The data are digitized in pairs to permit absolute timing between all slits. The electric field waveforms are also digitized at 2.5 MHz. This digitization rate yields an effective frequency response of ~1 MHz (recall that the tape recorder limit is 1 MHz at our recording speed). Examples of digitized optical waveforms are displayed in Fig. 8. The time differences between the beginning of faster portions of the rising waveforms (Fig. 8) are measured and then corrected for the systematic interchannel timing errors. The beginning of the faster portion of the optical signal is used because this point provides an easily determined and unambiguous point to measure all times. Other points on the optical waveform, i.e., peak or maximum slope, are not used in this analysis but could be used to measure the return-stroke velocity. From our preliminary analysis, however, these points tend to produce less consistent and lower return-stroke velocities than the start of the fast rise time.

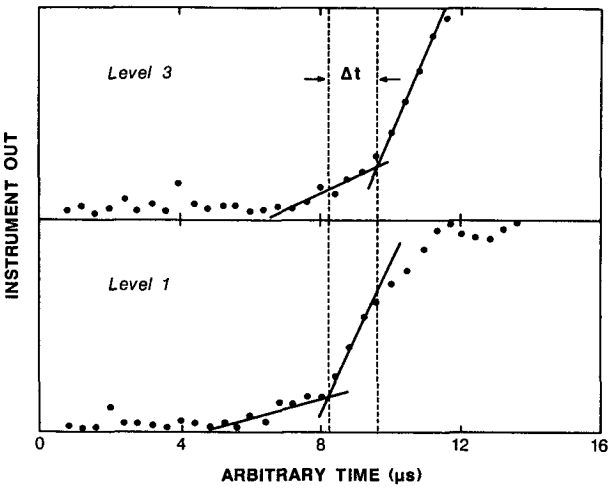

FIG. 8. RSV device voltage out versus time for levels one (the lowest) and three. The dashed vertical lines indicate the beginning of the faster rising portion of the optical pulses that are used for velocity determination. The time difference, Δt, is measured and corrected for systematic timing errors. Note that the signal from the third detector saturates the tape recorder but does not prohibit the velocity measurement.

We acquire the channel geometry from the video image, and the positions of the various slits on the image are determined from the calibration video recording. If the distance to the flash is less than about 5 km, there is usually a distinct thunder clap that can be used to estimate the distance. If no clap is heard, or if there are possible distance ambiguities because of other close lightning, we estimate the flash distance from cloud-base height, employing the lifted condensation level determined from the nearest atmospheric sounding. From a knowledge of the vertical field of view of the video camera, we determine the angular extent of the flash on the video image from the ground-strike point to where it enters the cloud. Using the cloud-base height and the flash angular extent, we determine the distance to the flash. A two-dimensional channel length is then calculated, and we determine the velocity between pairs of detectors. This procedure is performed for several different pairs of detectors, the choice of which depends on signal quality and video image clarity. Average velocities over large channel extents can be found by selecting nonadjacent pairs. Using various combinations of slit pairs, multiple velocity values are calculated along a single channel to determine velocity as a function of height.

4. Evaluation of RSV device capabilities and results

To understand the capabilities and limitations of the RSV device, we have analyzed 16 strokes that consist of three first-return strokes, nine subsequent-return

Unauthenticated | Downloaded 05/07/21 08:15 PM UTC

strokes, and four triggered-subsequent-return strokes. The strokes are divided evenly between each of our four major datasets. The four datasets consist of natural (nontriggered) lightning for the Great Plains (Oklahoma, North Texas and Southern Kansas), the Southeast (Alabama, Southern Tennessee and Florida), and triggered cloud-to-ground lightning in Florida. The velocities determined for these strokes vary from 1.2×10^8 m s^{-1} to 2.5×10^8 m s^{-1}. The accompanying timing uncertainties, and thus velocity uncertainties, range from 12%–35%, respectively. The other major source of error is in the distance to the flash, which we estimate to be about 15%–20% for the natural flashes and 10%–15% for the triggered ones. The average return stroke velocity over at least 500 m of channel near the ground is $1.7 \pm 0.8 \times 10^8$ m s^{-1} for these 16 strokes. These values are within the ranges reported previously (Idone and Orville 1982; Idone et al. 1984).

At the onset of this project, we were uncertain as to how results from the RSV device would compare with the established method using the streaking camera. Both systems were used to record triggered lightning in the summer of 1986 at Kennedy Space Center. Comparisons between velocities calculated from the same strokes indicate that the differences between the velocities calculated are less than the errors associated with each system (Idone et al. 1987).

The data for the RSV device are acquired in such a short interval that the motions and vibrations of the mobile laboratory should not affect data quality. To test this assumption, we recorded optical pulses and determined velocities from return strokes while the mobile laboratory was both moving and stationary. From our analysis, we find no differences between the characteristics of the pulse shape or the channel velocities calculated from them. Thus we feel confident in using results from data obtained while the RSV device is moving or stationary.

We find that there are limitations associated with the RSV device. One problem is that it is difficult to determine velocities from channels partially obscured by rain. Scattered light from these flashes slows and distorts the optical signal at each detector and makes it impossible to find the beginning of the fast transition used to calculate the velocity. Attempting to use the peak value of the optical pulse for these flashes does not solve the problem because the optical waveforms from each detector level are distorted by rain-scattered light so that the optical signal is no longer from a 1–5 m channel segment but from a large section of the channel. A return-stroke velocity measurement between slit levels, therefore, can not be made. Velocities determined from the peak light intensity from flashes not obscured by rain are usually slower than those determined from the initial fast rise in the return stroke due to the slowing of the risetime of the optical signal with height (Jordan and Uman 1983). The major limitation of our RSV system is that we can not determine the interval between pulses to a better timing accuracy than about 0.2 μs owing to tape recorder jitter at a recording speed of 60 ips.

5. Conclusions

In its present form, our RSV device produces results similar to the ones obtained with the streaking camera. It has added advantages of a significantly smaller size, much lower cost, mobile use, and easier data collection and analysis. Although solid-state detector systems have been used before to measure return-stroke velocities, our version is unique because it allows more than one velocity value to be obtained along the channel. The maximum accuracy of 0.2 μs for the RSV is four times better than the maximum accuracy of about 0.8 μs associated with the streaking camera (Idone et al. 1987). In addition, the errors associated with the RSV device can be lowered further by using a digital recording method or jitter-removing system (Mach 1987). We now have the means to acquire a large database of return-stroke and leader velocities.

Acknowledgments. We gratefully acknowledge the contributions of the crew of the mobile laboratory: Dr. Robert Davies-Jones, who provided storm intercept strategies; Brian Curran, who drove skillfully in adverse conditions; and Lance Scudder, who assembled much of the instrumentation and did real-time quality control of the electric field change data. We would like to thank Dr. E. Philip Krider for the invitation to participate in the Florida triggered-lightning experiment at Kennedy Space Center and Dr. Charles Weidman for collecting most of the mobile laboratory data there. Kevin Cameron designed the operational amplifier circuit used in the RSV device. We thank Dr. Hugh Christian and Steve Goodman for supporting our participation in COHMEX.

This research was supported in part by the Severe Storms and Local Weather Research Office of NASA under Government order H-39299B.

REFERENCES

Boyle, J. S., and R. E. Orville, 1976: Return stroke velocity measurements in multistroke lightning flashes. *J. Geophys. Res.*, **81**, 4461–4466.

Hubert, P., and G. Mouget, 1981: Return stroke velocity measurements in two triggered lightning flashes. *J. Geophys. Res.*, **86**, 5253–5261.

Idone, V. P., and R. E. Orville, 1982: Lightning return stroke velocities in the Thunderstorm Research International Program (TRIP). *J. Geophys. Res.*, **87**, 4903–4915.

——, ——, P. Hubert, L. Barret and A. Eybert-Berard, 1984: Correlated observations of three triggered lightning flashes. *J. Geophys. Res.*, **89**, 1385–1394.

——, ——, D. M. Mach and W. D. Rust, 1987: The propagation speed of a positive return stroke. *Geophys. Res. Lett.*, **14**, 1150–1153.

Jordan, D. M., and M. A. Uman, 1983: Variation in light intensity with height and time from subsequent lightning return strokes. *J. Geophys. Res.*, **88**, 6555–6562.

Kawasaki, Z. I., M. Nakano, T. Takeuti and T. Nakai, 1985: Group

Unauthenticated | Downloaded 05/07/21 08:15 PM UTC

velocities of lightning return stroke currents. *10th International Aerospace and Ground Conference on Lightning and Static Electricity,* Paris, France, 241–245. [Available from Les Editions de Physique, Avenue du Hoggar, Zone Industrielle de Courtaboeuf, B.P. 112, 91944 Les Ulis Cedex, France.]

Leise, J. A., and W. L. Taylor, 1977: A transmission line model with general velocities for lightning. *J. Geophys. Res.,* **82,** 391–396.

Lin, Y. T., M. A. Uman and R. B. Standler, 1980: Lightning return stroke models. *J. Geophys. Res.,* **85,** 1571–1583.

Lundholm, R., 1957: Induced overvoltage surges on transmission lines. *Chalmer Tek. Hoegsk. Handl.,* **188,** 1–117.

MacGorman, D. R., M. W. Maier and W. D. Rust, 1984: Lightning strike density for the contiguous United States from thunderstorm duration records. *Report to the U. S. Nuc. Reg. Com., NUREG/CR 3759,* 44 pp. [NTIS, Springfield, VA, 22161.]

Mach, D. M., 1987: Return stroke velocities and currents using a solid state silicon detector system. PhD. thesis, The University of Oklahoma, Norman, Oklahoma. 93pp. [Available from University Microfilms, Ann Arbor, Michigan.]

Master, M. J., M. A. Uman, Y. T. Lin and R. B. Standler, 1981: Calculations of lightning return stroke electric and magnetic fields above ground. *J. Geophys. Res.,* **86,** 12 127–12 132.

McEachron, K. B., 1939: Lightning to the Empire State Building. *J. Franklin Inst.,* **227,** 149–217.

Orville, R. E., G. G. Lala and V. P. Idone, 1978: Daylight time resolved photographs of lightning. *Science,* **201,** 59–61.

Radda, G. J., and E. P. Krider, 1974: Photoelectric measurements of lightning return stroke propagation speeds (abstract). *Eos Trans. AGU,* **56,** 1131.

Schonland, B. F. J., and H. Collens, 1934: Progressive lightning, 1. *Proc. Roy. Soc. London,* **143,** 654–574.

——, D. J. Malan and H. Collens, 1935: Progressive lightning, 2. *Proc. Roy. Soc. London,* **152,** 595–625.

Uman, M. A., and D. K. McLain, 1969: Magnetic field of lightning return stroke. *J. Geophys. Res.,* **74,** 6899–6909.

——, ——, R. J. Fisher and E. P. Krider, 1973: Currents in Florida lightning return strokes. *J. Geophys. Res.,* **78,** 3530–3537.

——, ——, and E. P. Krider, 1975: The electromagnetic radiation from a finite antenna. *Am. J. Phys.,* **43,** 33–38.

Unauthenticated | Downloaded 05/07/21 08:15 PM UTC